

Observation and Structural Determination of $(\sqrt{3} \times \sqrt{3})R30^\circ$ Reconstruction of the Si(111) Surface

W. C. Fan and A. Ignatiev

Department of Physics and Space Vacuum Epitaxy Center, University of Houston, Houston, Texas 77204

H. Huang

Department of Physics and Laboratory for Surface Studies, University of Wisconsin-Milwaukee, Milwaukee, Wisconsin 53201

S. Y. Tong^(a)

National Science Foundation, 1800 G Street, N. W., Washington, D.C. 20550

(Received 12 December 1988)

A new reconstruction structure, having a $(\sqrt{3} \times \sqrt{3})R30^\circ$ unit cell, is reported for the Si(111) surface. Analysis of low-energy electron-diffraction intensity spectra by multiple-scattering theory revealed a vacancy model. The bonds between the first- and second-layer atoms are of the sp^2 type, resulting in a highly compressed surface bilayer. Measured intensity spectra of the clean and Ag-deposited $(\sqrt{3} \times \sqrt{3})R30^\circ$ surfaces are very similar. This leads us to conclude that the Ag-Si interface is not sharp and that the Ag atoms do not form a lattice structure that has long-range ordering.

PACS numbers: 68.35.Bs

The reconstruction structures of the Si(111) surface have been studied since the beginning of surface science.^{1,2} It has been well established that on Si(111), there is an annealed (7×7) structure and a room-temperature cleaved (2×1) structure. In this Letter, we report the observation of a third reconstruction structure. The new structure has a $(\sqrt{3} \times \sqrt{3})R30^\circ$ periodicity [hereafter referred to as Si(111)- $\sqrt{3}$]. Using low-energy electron diffraction, we have measured intensity-voltage (IV) spectra for this surface and analyzed the data by the multiple-scattering LEED method. The analysis revealed a vacancy model which involves substantial normal compression of the top bilayer and large lateral displacements of the second plane of atoms, in a formation analogous to that found on the (2×2) GaAs(111) surface.^{3,4}

We have also deposited Ag atoms on Si(111) and measured the IV spectra of the Si(111) $(\sqrt{3} \times \sqrt{3})R30^\circ$ -Ag surface [hereafter referred to as Si(111)- $\sqrt{3}$ -Ag]. The Si(111)- $\sqrt{3}$ -Ag system is one that has been studied by almost every surface technique,⁵ but there is still no consensus about the atomic arrangement of the Ag and Si atoms. Our comparison of the IV spectra for different beams showed that they are extremely similar to those of the clean Si(111)- $\sqrt{3}$ surface. This leads us to conclude that the Ag-Si interface is not sharp. There is substantial intermixing between the Ag and Si atoms; however, the Ag atoms *do not form a lattice structure that has a long-range order*. The ordered honeycomb patterns observed by scanning tunneling microscopy (STM) are the Si surface atoms of the vacancy structure.^{6,7}

The experiments were carried out in an ultrahigh-vacuum (UHV) chamber with a four-grid LEED optics as described previously.⁸ The LEED optics were also used as a retarding-field analyzer for Auger-electron

spectroscopy (AES). The IV curves were measured from the LEED optics with a high-sensitivity video camera interfaced to a personal computer. The sample was cut from a silicon single-crystal block and aligned with x-ray diffraction to expose the (111) surface to better than 0.2° . The sample surface was then polished with Al_2O_3 polishing paste, before mounting onto a holder connected to a UHV manipulator. The silver source for deposition was a piece of tungsten wire with a silver bead at the center, located at about 10 cm away from the sample. The evaporation of Ag in the experiments was controlled at a rate of 0.1 ML/min (1 ML = 7.8×10^{14} atom/cm²) as calibrated by a quartz microbalance next to the sample. The vacuum condition of the chamber was maintained at better than 2×10^{-10} Torr for the period of the experiments.

The Si(111) sample was first intensely bombarded (dose $\approx 10^{18}$ ions/cm²) with 1-keV Ar ions so that a clean surface, but with multilayer damage, was obtained. After the Ar⁺ bombardment, the Si crystal was rapidly heated ($10^\circ C/sec$) up to $1000^\circ C$ for annealing and then rapidly cooled ($20^\circ C/sec$). The damaged Si(111) surface underwent an order-disorder reconstruction process which is a function of the annealing time. A $(\sqrt{3} \times \sqrt{3})R30^\circ$ pattern was observed from the Si(111) surface after a 5-sec annealing at $1000^\circ C$. This is shown in Fig. 1(a). With increased annealing time, this $(\sqrt{3} \times \sqrt{3})$ pattern became weaker and some weak "streaks" appeared in the diffraction patterns [Figs. 1(b) and 1(c)]. Further increase of annealing time at $1000^\circ C$ resulted in the disappearance of the $(\sqrt{3} \times \sqrt{3})$ pattern [Fig. 1(d)] with the streaks becoming more defined as diffraction spots of the (7×7) structure. The streaks, therefore, may indicate a local (7×7) reconstruction.

The observed $(\sqrt{3} \times \sqrt{3})$ phase, therefore, results from

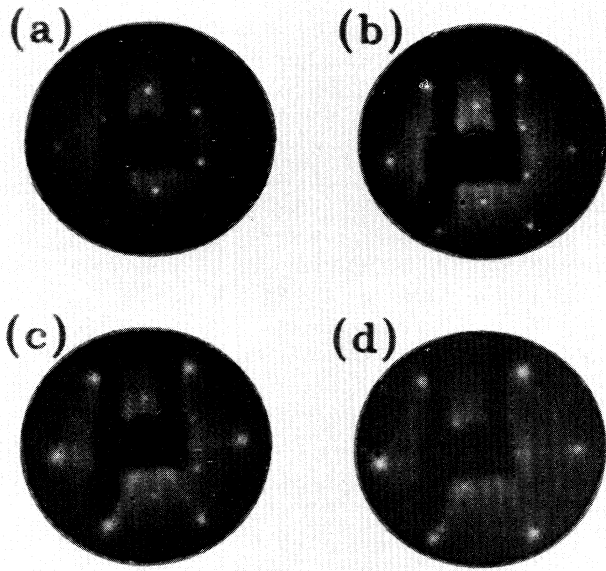


FIG. 1. LEED patterns at room temperature after Ar^+ (1 keV) bombardment and annealing at 1000°C for (a) 5 sec, (b) 10 sec, (c) 20 sec, and (d) 1 min, and at (a) 41 eV, (b) 47 eV, (c) 46 eV, and (d) 44 eV. The integral-order spots are the ones farthest from the origin in each pattern.

the reconstruction of the damaged top layers of the Si(111) surface. This $(\sqrt{3}\times\sqrt{3})$ structure is less stable than the (7×7) structure of Si(111) at high temperature, but at room temperature, it is quite stable and is maintained even for several days. The $(\sqrt{3}\times\sqrt{3})$ structure is reproducible and does not seem to be based on specific contamination at the surface, as AES showed no indication of contamination (see Fig. 2). It is however possible, though unlikely, that this $(\sqrt{3}\times\sqrt{3})$ reconstruction of the Si(111) surface might be affected by a residual impurity ($< 1\%$) of Ar implanted into the silicon sample during the bombardment and possibly not desorbed by the short annealing. The very short annealing time required to form this structure is probably why it has not been found until now.

The measured IV spectra for the clean Si(111)- $\sqrt{3}$ structure were compared with calculated curves generated from a new-generation multiple-scattering LEED code which included symmetries in real⁹ and reciprocal spaces.^{10,11} The dynamical inputs are identical to those used for the analysis of the Si(111) (7×7) surface.^{12,13} The calculations used seven phase shifts and an inner potential of 12 eV. We tested previously suggested models and new models. The analysis found that a vacancy model produced calculated IV curves in best agreement with the measured data. All the previously suggested models can be ruled out in comparison with the vacancy model proposed here. Figure 3 shows a top view of the clean Si(111)- $\sqrt{3}$ vacancy model. In this model, a first-layer Si atom in each $\sqrt{3}\times\sqrt{3}$ unit cell is missing. The

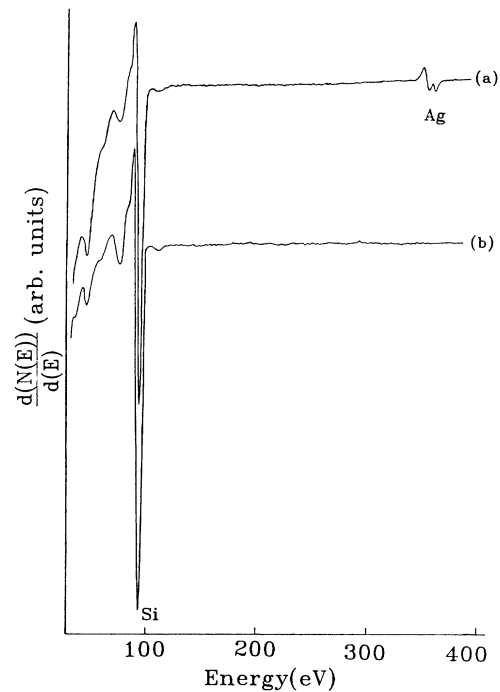


FIG. 2. Auger-electron spectroscopy, curve *a*, from the $(\sqrt{3}\times\sqrt{3})$ structure of the Si(111) surface with about 1-ML Ag exposure, and curve *b*, from the clean Si(111) with the $(\sqrt{3}\times\sqrt{3})R30^\circ$ structure.

vertical spacing between the first- and second-layer atoms (i.e., the first bilayer distance) is highly compressed, to 0.28 Å from the bulk value of 0.78 Å. The three second-layer Si atoms in the $\sqrt{3}\times\sqrt{3}$ unit cell are displaced laterally along the arrows of Fig. 3 by 0.65 Å. The vertical distance between second- and third-layer atoms is 2.28 Å (bulk value is 2.35 Å). The vertical dis-

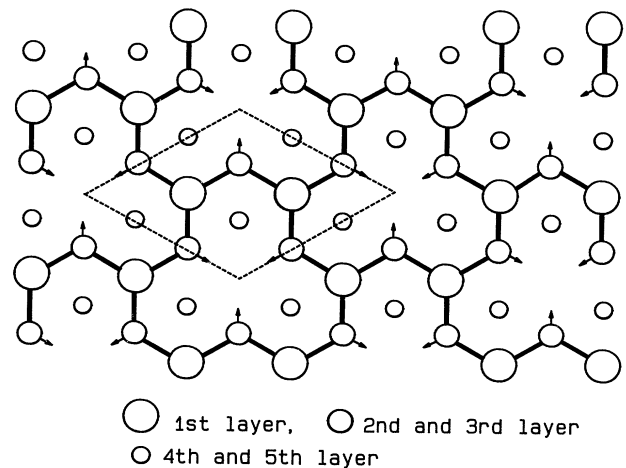


FIG. 3. Schematic top view diagram of the vacancy model. The broken lines denote the $(\sqrt{3}\times\sqrt{3})R30^\circ$ unit cell.

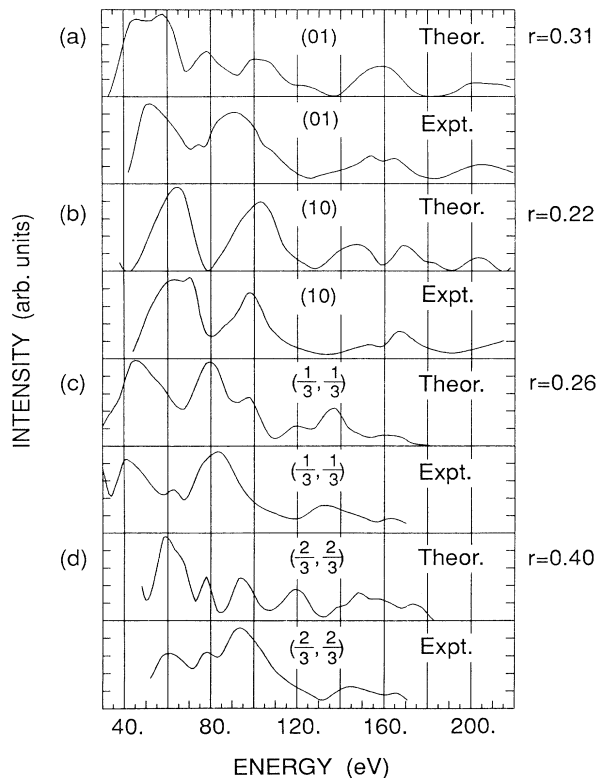


FIG. 4. Comparison between theory and experiment for the vacancy model. r , individual-beam R factor; $\theta=0^\circ$.

tance between third and fourth layers (i.e., second bilayer distance) is 0.64 \AA . The atoms in the third layer are laterally displaced along the arrows of Fig. 3 by 0.24 \AA . All other atomic coordinates are found to be at bulk sites. Figure 4 shows the comparison of IV spectra at normal incidence between experiment and theory for the vacancy model. The Van Hove-Tong R factor averaged over the four beams is 0.29 .

It would be interesting to consider the electronic rehybridization for this model. The bonds between the first- and second-layer atoms rehybridize from sp^3 to sp^2 , leaving the dangling bonds of the surface Si atoms essentially empty. The planar nature of the sp^2 bonds explains why the first bilayer distance is compressed to 0.28 \AA , while the second-layer atoms are laterally displaced by 0.65 \AA . With $\frac{1}{3}$ -ML vacancies, the dangling bonds on the second-layer Si atoms are not completely filled. Thus, we expect roughly 8% of the surface not to have vacancies. This lack of complete ordering explains the following: (i) The clean $\text{Si}(111)-\sqrt{3}$ structure is not very stable under annealing. The structure becomes 7×7 upon annealing at 1000°C beyond 5 sec. (ii) The long-range order of this structure is relatively poor. The diffuse background in the LEED pattern is quite high. We expect this structure to have increased stability and its

long-range order improved by deposition of metal atoms that contribute one electron per $\sqrt{3} \times \sqrt{3}$ unit cell, i.e., at a metallic coverage of 0.3 ML or more.

We now turn to the deposition of Ag atoms on $\text{Si}(111)$. Before the evaporation of silver, the $\text{Si}(111)$ sample was annealed at 1000°C for 3 min and cooled down to 500°C , so that a clear (7×7) LEED pattern was observed. As a function of the Ag exposure, the (7×7) pattern first became very weak and diffuse similar to that in Fig. 1(d). At an Ag exposure of about 0.3 ML, a $(\sqrt{3} \times \sqrt{3})$ pattern with intensity streaks appeared, which was like the one shown in Fig. 1(c). After the exposure reached about 0.6 ML, the LEED pattern of the $(\sqrt{3} \times \sqrt{3})$ structure of Ag on $\text{Si}(111)$ became very clear, and it has higher contrast and lower diffuse background than that of the $(\sqrt{3} \times \sqrt{3})$ structure of the clean $\text{Si}(111)$ surface.

Figure 5 shows the measured LEED IV curves of the $(\sqrt{3} \times \sqrt{3})$ structures discussed above. The IV curves for the $(\sqrt{3} \times \sqrt{3})$ structure of Ag on $\text{Si}(111)$ are shown as curves *a*, while those of the $(\sqrt{3} \times \sqrt{3})$ phase of clean $\text{Si}(111)$ formed after the 5-sec annealing are shown as curves *b*. The similarities of the two sets of curves are rather striking. LEED IV curves are sensitive to atomic arrangements with long-range order. Since the IV curves for $\text{Si}(111)-\sqrt{3}\text{-Ag}$ remain unchanged even when multilayers of Ag are deposited on the surface, we are led to the conclusion that the Ag atoms do not form lattice structures that have a long-range order. The Ag atoms, however, play a role in stabilizing the $\text{Si}(111)$ vacancy model. Earlier work by Yang, Wu, and Jona¹⁴ on $\text{Si}(111) (\sqrt{3} \times \sqrt{3})R30^\circ\text{-Ta}$ has found similar IV curves for the Ag and Ta covered surfaces. We expect that Ag and Ta play a similar role and that both metals stabilize the $\text{Si}(111)-\sqrt{3}$ vacancy structure. A corollary of this picture is the prediction that a STM scan of the $\text{Si}(111) (\sqrt{3} \times \sqrt{3})R30^\circ\text{-Ta}$ surface should reveal a similar honeycomb pattern and that this pattern is due to electronic orbitals centered on the surface Si atoms. Recent works of $\text{Si}(111) (\sqrt{3} \times \sqrt{3})R30^\circ\text{-Ga}$ ¹⁵ and -Pb ¹⁶ showed that the Ga and Pb atoms formed ordered overlayers on the $\text{Si}(111)$ substrate. As a consequence, we expect the IV curves of these two systems to be very different from one another and also different from those of the clean $\text{Si}(111)-\sqrt{3}$ vacancy structure. An inspection of the IV curves confirmed this expectation.

In summary, we have uncovered a stable $(\sqrt{3} \times \sqrt{3})$ structure on the clean $\text{Si}(111)$ surface and explained the structure in terms of a surface vacancy model. The driving mechanism for stabilizing this vacancy model is similar to that found earlier on $\text{GaAs}(111)$.^{3,4} This may seem surprising since $\text{Si}(111)$ is monatomic while $\text{GaAs}(111)$ is diatomic. However, similar Jahn-Teller distortions have been found in the buckled dimers of the $\text{Si}(100)$ surface.¹⁷ The $\text{Si}(111)-\sqrt{3}\text{-Ag}$ structure is explained in terms of the Ag metal atoms stabilizing the

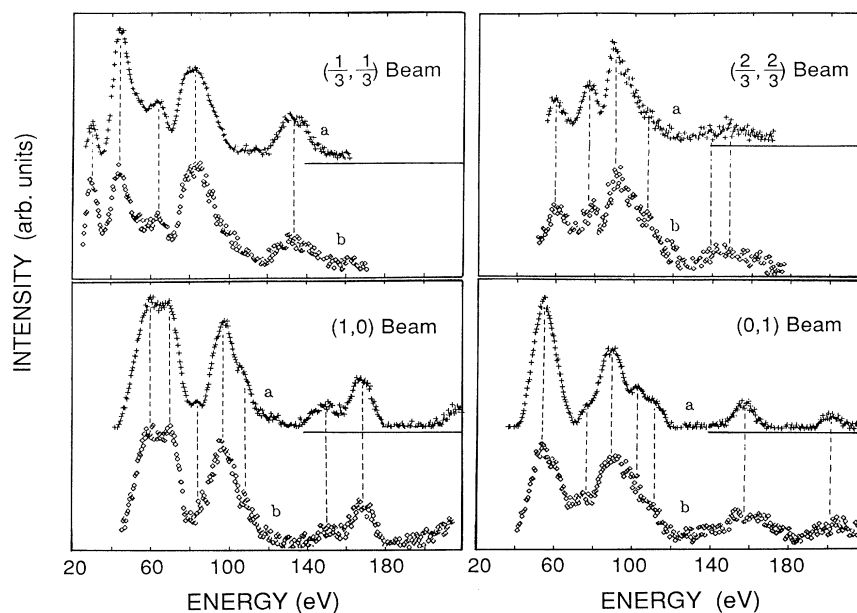


FIG. 5. Measure normal incidence IV curves for the $(\sqrt{3}\times\sqrt{3})R30^\circ$ structures for, curves *a*, Ag on Si(111) and, curves *b*, clean Si(111) after Ar^+ bombardment and 5-sec annealing at 1000°C .

clean Si(111)- $\sqrt{3}$ vacancy structure while the Ag atoms themselves do not form structures with long-range order.

The assistance of J. Strozier with computer software for the data acquisition is acknowledged. This work is supported in part by the R. A. Welch Foundation, by NASA, and by the National Science Foundation, Grant No. DMR-8805938.

^(a)Permanent address: Laboratory for Surface Studies and Department of Physics, University of Wisconsin, Milwaukee, WI 53201.

¹R. F. Schlier and H. E. Farnsworth, *J. Chem. Phys.* **20**, 917 (1959).

²J. J. Lander, G. W. Gobeli, and J. Morrison, *J. Appl. Phys.* **34**, 2298 (1963).

³S. Y. Tong, G. Xu, and W. N. Mei, *Phys. Rev. Lett.* **52**, 1693 (1984).

⁴D. J. Chadi, *Phys. Rev. Lett.* **52**, 1911 (1984).

⁵An extensive reference list can be found in J. H. Huang and R. S. Williams, *Phys. Rev. B* **38**, 4022 (1988).

⁶E. J. Van Loenen, J. E. Demuth, R. M. Tromp, and R. J. Hamers, *Phys. Rev. Lett.* **58**, 373 (1987).

⁷R. J. Wilson and S. Chiang, *Phys. Rev. Lett.* **58**, 369 (1987).

⁸W. C. Fan, J. Strozier, and A. Ignatiev, *Surf. Sci.* **195**, 226 (1988).

⁹W. Moritz, *J. Phys. C* **17**, 353 (1984).

¹⁰M. A. Van Hove and J. B. Pendry, *J. Phys. C* **8**, 1362 (1975).

¹¹J. Rundgren and A. Salwen, *Comput. Phys. Commun.* **9**, 312 (1975).

¹²S. Y. Tong, H. Huang, C. M. Wei, W. E. Packard, F. K. Men, G. Glander, and M. B. Webb, *J. Vac. Sci. Technol. A* **6**, 615 (1988).

¹³H. Huang, S. Y. Tong, W. E. Packard, and M. B. Webb, *Phys. Lett. A* **130**, 166 (1988).

¹⁴W. S. Yang, S. C. Wu, and F. Jona, *Surf. Sci.* **169**, 383 (1986).

¹⁵A. Kawazu and H. Sakama, *Phys. Rev. B* **37**, 2704 (1988).

¹⁶H. Huang, C. M. Wei, H. Li, B. P. Tonner, and S. Y. Tong, *Phys. Rev. Lett.* **62**, 559 (1989).

¹⁷D. J. Chadi, *J. Vac. Sci. Technol.* **18**, 856 (1981).

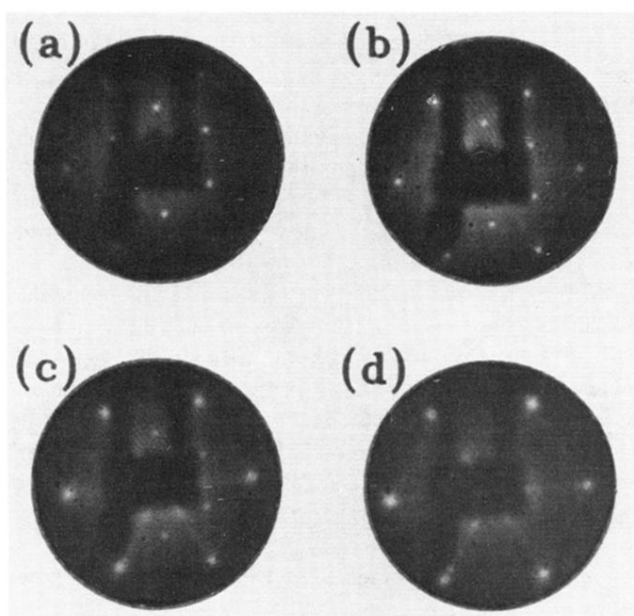


FIG. 1. LEED patterns at room temperature after Ar^+ (1 keV) bombardment and annealing at 1000°C for (a) 5 sec, (b) 10 sec, (c) 20 sec, and (d) 1 min, and at (a) 41 eV, (b) 47 eV, (c) 46 eV, and (d) 44 eV. The integral-order spots are the ones farthest from the origin in each pattern.